

Article

Mechanical, Morphological, and Electrical Characteristics of Cu-Loaded Acrylic Paint on a Fused Deposition Modeling Printed Polylactic Acid Surface

Sudhir Kumar ^{1,*}, Pulkit Tiwari ² and Seyed Saeid Rahimian Koloor ^{3,4,*}

¹ Department of Mechanical Engineering, Thapar Institute of Engineering and Technology, Patiala 147004, Punjab, India

² Information System, Jindal Global Business School, O.P. Jindal Global University, Sonapat 131001, Haryana, India; pulkitcdacnoida@gmail.com

³ Faculty of Mechanical Engineering, Universität der Bundeswehr München, Werner-Heisenberg-Weg 39, 85579 Neubiberg, Munich, Germany

⁴ Institute for Nanomaterials, Advanced Technologies and Innovation, Technical University of Liberec, Studentská 2, 461 17 Liberec, Czech Republic

* Correspondence: sudhirdwivedi1992@gmail.com (S.K.); seyed.rahimian@unibw.de (S.S.R.K.)

Abstract: Fused deposition modeling (FDM) printing has become increasingly popular for exploring advanced material matrices with a polymeric base. This study uses a low-energy method to investigate the metallization process on a surface created by 3D printing. This involves using an acrylic-paint-based solution to disperse the copper (Cu) powder on a polylactic acid (PLA) substrate, allowing for an evaluation of the fabricated samples' mechanical, morphological, absorbance, and capacitance properties. The study findings indicate a gradual increase in tensile strength as the content of Cu in the acrylic paint layer on the PLA substrate increases. There was a clear and consistent increase in the tensile strength of the specimen, ranging from 13.5 MPa (sample 1) to 15.6 MPa (sample 5). Similarly, the percentage of strain at failure also showed a noticeable increase, ranging from 4.2% (sample 1) to 8.6% (sample 5). The scanning electron microscopy (SEM) investigation revealed the presence of completely enveloped Cu particles in acrylic paint on the FDM-printed surface of the PLA. The Ultraviolet–Visible Diffuse Reflectance Spectroscopy (UV–Vis DRS) indicated a significant change in the absorbance pattern as the copper content in the layer increased. The augmented absorbance values serve as an advantage because they demonstrate enhanced UV light interaction, which correlates with the increase in capacitance measurements of 6 to 8 pF. This result suggests that the fabricated sample potentially leads to favorable alterations in material characteristics for applications that demand stable capacitance alongside improved mechanical properties. The SEM analysis supported the observed trends.

Keywords: 3D printing; material characterization; composite fabrication; UTM testing; SEM analysis



Academic Editors: Md Nizam Uddin and Faycal Znidi

Received: 24 February 2025

Revised: 31 March 2025

Accepted: 31 March 2025

Published: 2 April 2025

Citation: Kumar, S.; Tiwari, P.; Rahimian Koloor, S.S. Mechanical, Morphological, and Electrical Characteristics of Cu-Loaded Acrylic Paint on a Fused Deposition Modeling Printed Polylactic Acid Surface. *Processes* **2025**, *13*, 1059. <https://doi.org/10.3390/pr13041059>

Processes **2025**, *13*, 1059. <https://doi.org/10.3390/pr13041059>

Copyright: © 2025 by the authors. Licensee MDPI, Basel, Switzerland. This article is an open access article distributed under the terms and conditions of the Creative Commons Attribution (CC BY) license (<https://creativecommons.org/licenses/by/4.0/>).

1. Introduction

The manufacturing of lightweight composite materials and structures with enhanced mechanical performance is a key focus in research and development, utilizing advanced methods like automated fabrication and 3D printing [1]. Additive manufacturing (AM) and 3D printing are recognized as sustainable methods that minimize waste and offer cost-effectiveness, along with design flexibility for complex structures, although further research

is needed for product optimization [2–5]. To enhance the mechanical, morphological, thermal, and other properties of 3D-printed components, fused deposition modeling (FDM), a prominent AM technique, has explored various material and process factors [6]. However, FDM faces challenges in material compatibility and processing, which have been partially addressed by integrating post-processing techniques over the last five years, improving attributes such as surface smoothness, thermal and chemical stability, and electrical conductivity of polymeric substrates.

Vinay et al. [7] reported that reinforcing PLA with 10–20 wt% aluminum (Al) powder improved tensile strength and hardness by 57% and 28.5%, respectively, although ductility decreased. A tensile strength of 31.20 MPa was achieved with 20 wt% Al, surpassing virgin PLA's 21.30 MPa. Fijol et al. [8] found polysaccharide nanofiber composites to be 54% more effective than pure PLA filters in micro-plastic removal and effective in metal ion adsorption. Sadeghian et al. [9] analyzed Cu-reinforced PLA, noting a 15.9% tensile strength increase in flat orientation. Hasanzadeh et al. [10] indicated reduced mechanical strength and ductility with Al particles. Kam et al. [11] studied PLA/20%Cu and PLA/20%Bronze for vibration damping, finding Cu reinforcement most effective in reducing vibration amplitude. Petousis et al. [12] incorporated 4.2 wt% titanium nitride (TiN) into a polylactic acid (PLA) matrix, achieving a 51% increase in flexural strength and a 43% rise in tensile strength. Yelamanchi et al. [13] studied fiber metal laminates with aluminum alloy, reporting a 9–13% enhancement in fracture strength. Raichur et al. [14] investigated PLA reinforced with 10 wt% nano clay, finding reduced wear due to improved shear friction properties. Mansour et al. [15] enhanced PLA strength using nano diamonds (NDs) and carbon fiber (CF), with PLA/ND showing an elastic modulus of 6250 MPa, significantly higher than virgin PLA's 2684 MPa, and a 106% increase in vibration damping. Fijot et al. [16] evaluated a PLA/TCNF substrate with SU-101 metal organic framework (MOF) for water treatment, demonstrating an improved filtering performance and a Young's modulus increase to 1200 MPa.

Paz-Gonzalez et al. [17] studied PLA/CF composites for bone replacement, achieving a tensile strength of 238 MPa and 80% cell viability, comparable to bone strength. Ambrus et al. [18] examined FDM parameters for PLA/Cu filaments, noting a peak tensile stress of 9.32 MPa in horizontally built objects. Bodaghi et al. [19] added E-glass fibers to ABS to enhance wear resistance in gears, resulting in improved thermomechanical properties. Mohammadi-Zerankeshi and Alizadeh [20] explored the effects of magnesium (Mg) in PLA/graphene composites, finding a mechanical strength increase to 50 MPa from 42 MPa and a transformation to a hydrophilic surface. Sharif et al. [21] developed a method for Cu plating on polymer substrates via electroless plating, which led to a significant reduction in PLA's mechanical properties, with tensile strength dropping to 65%, while tensile modulus increased by 63%, and elongation at break improved by 25%.

Kumar et al. [22] investigated steel-coated PLA samples using electric arc spray, recommending a 100 μm thickness for optimal mechanical properties, achieving a tensile strength of 29 MPa, corrosion rate of 0.055 mm/year, and wear rate of 0.11. Moraczewski et al. [23] explored electroless copper plating on PLA pre-coated with tannic acid and polydopamine, enhancing the electrical properties by reducing surface resistivity from 10^{11} – 10^{14} Ω to 10^4 – 10^5 Ω . Inclán-Sánchez [24] assessed a 3D-printed antenna using a substrate-free metal mesh, modified with conductive paint. Aziz et al. [25] reviewed various studies on 3D FDM printing for antennas across disciplines, including SATCOM. Farajian et al. [26] analyzed PU/MWCNT coatings on PLA, noting an increase in tensile strength from 30 MPa to 40 MPa in typical environments but a decrease to 28 MPa after 30 days in a NaCl corrosive environment. Ekonomou et al. [27] studied the antibacterial effects of Silver (Ag) and Copper (Cu) coatings on PLA and TPU, finding that these coatings

enhanced hydrophobicity and reduced bacterial colonization. Moradi et al. [28] explored iron-filled PLA in 4D printing, revealing that samples printed with a magnet beneath the surface achieved a 63.5% increase in magnetization and a maximum tensile stress of 14 MPa. Sukindar et al. [29] focused on the surface roughness of PLA-Al feedstock, noting that the FDM process maintained dimensional stability with only a 5% deviation. Alzyod et al. [30] investigated ironing as a post-processing technique, achieving a significant reduction in surface roughness from 8–10 Ra to 1–1.5 Ra for PLA samples, influenced by factors like path speed and flow rate. Amin et al. [31] examined chemical etching of PLA to create superhydrophobic surfaces, utilizing pyramid structures and the staircase effect from FDM printing.

Scope for the Present Work

It appears from the literature survey that PLA can be fused with a variety of metallic and non-metallic materials with the assistance of aluminum powder, copper, titanium nitride, carbon fiber, graphene–magnesium, and polysaccharide nanofibers to enhance several properties of PLA—mainly tensile strength, flexural strength, hardness, thermal stability, and electrical conductivity. For instance, works by Vinay et al. [7] and Kam et al. [11] established improvements in mechanical performance characteristics of the PLA reinforced with aluminum and copper, whereas these by Mansour et al. [15] and Sadeghian et al. [9] advanced the mechanical features of PLA through carbon fiber and copper reinforcement. Moreover, investigations carried out by Petousis et al. [12] and Moradi et al. [28] brought to relief an appreciable improvement in electrical conductivity and antibacterial activity of PLA using materials like titanium nitride and copper. Studies conducted by Raichur et al. [14] and Sharif et al. [21] have stressed the significance of nanomaterials plus metallic reinforcements concerning the tribological and wear resistance features of PLA. Even though there exists copious literature on the reinforcement of PLA, there are not many papers on metallization methods that do not imply the use of high-energy techniques or hazardous chemicals. This study aims to fill this gap by conducting further work on low-energy and environmentally friendly metallization of PLA surfaces through functionalizing copper powder with acrylic paint residue binder. The intent is to report the mechanical, morphological, and electrical properties of PLA while keeping the energy expense low and environmentally friendly during metallization, typically avoiding excess chemical treatments or high-energy input required.

2. Materials and Methods

2.1. Material Selection and Sample Preparation

For the preparation of samples, commercial feedstock filament of PLA was purchased from Dream Polymer Group, Gujarat, India. The copper nano powder of 325 mesh size was procured from AUM industry, Gujrat, India. Similarly, acrylic paint (Make: PIDILITE Industries Limited; Maharashtra, India; acrylic color: white) was purchased through local vendor Ahuja paint shop, Patiala, Punjab, India. In the first stage, samples of ASTM D638 Type IV for mechanical UTM testing, a rectangular specimen of $15 \times 15 \text{ mm}^2$ size for conductivity and UV–Vis diffuse reflectance spectroscopy testing (UV–Vis DRS) was FDM-printed using the standard printing procedure with the settings given in Table 1. Figure 1 shows the workflow/methodology for the current research investigation.

Table 1. FDM printing standard settings.

Machine Parameters	Value
Base temperature	65 °C
Nozzle temperature	210 °C
Infill percentage	10%
Number of layers	4
Infill orientation	45 degrees
Infill pattern	Linear

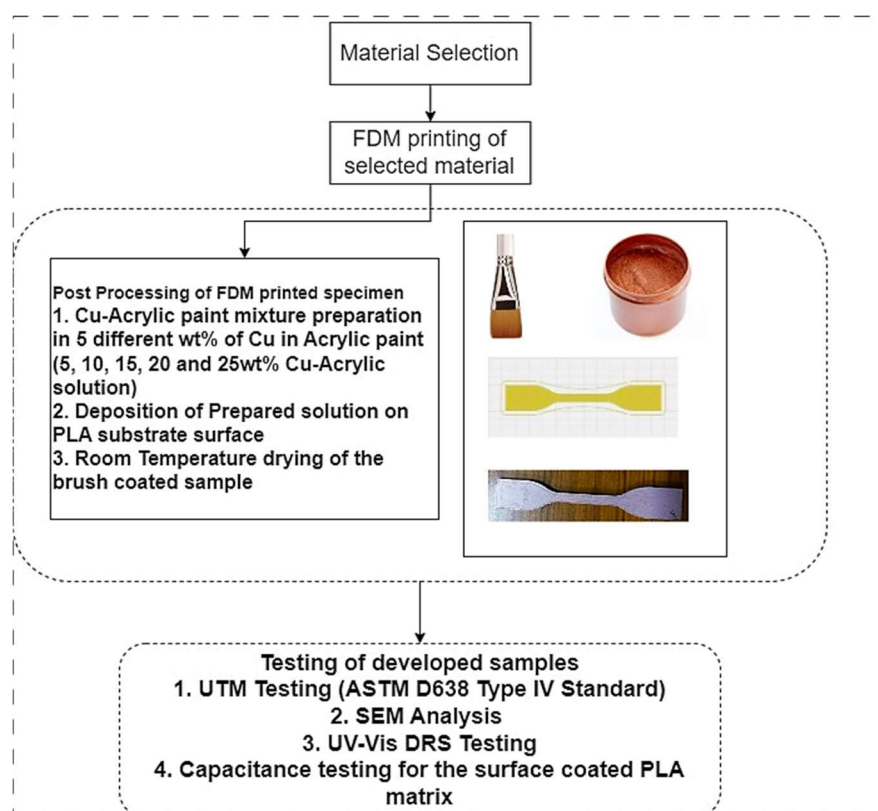
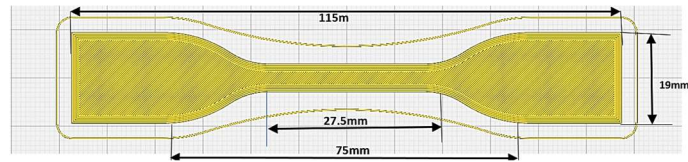
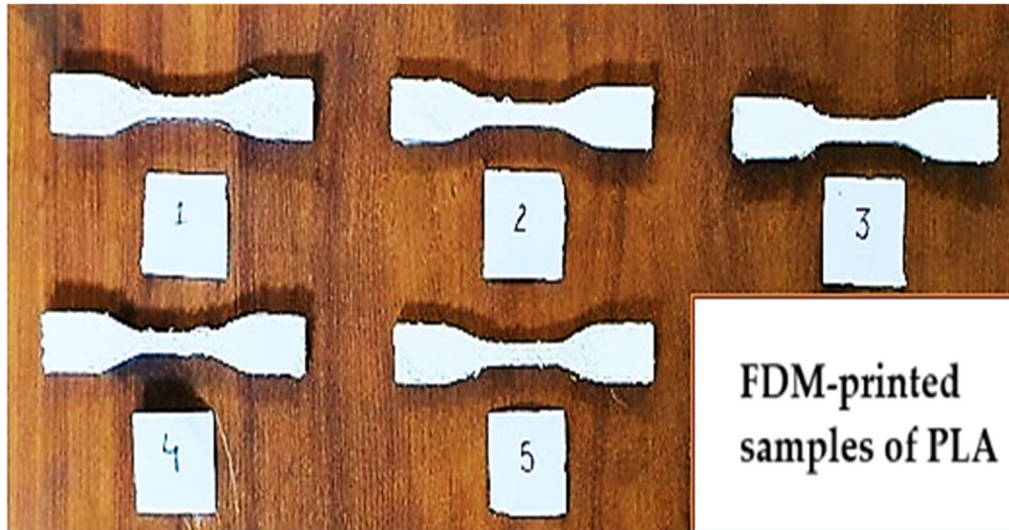
**Figure 1.** Selected workflow for the current research investigation.

Figure 2 shows the samples of PLA: (a) sliced image for tensile sample; (b) tensile sample printed with ASTM D638 Type IV standard size; (c) Cu-coated sample; and (d) 15 × 15 mm samples of PLA coated with Cu powder for UV-Vis DRS and conductivity testing. In this study, 5 samples were printed (3 repetitions for each sample for standard deviation calculation) with the standard printing procedure as given in Table 1. Following FDM printing operations, PLA samples received surface applications of acrylic paint containing five distinct Cu ratios (5 wt%, 10 wt%, 15 wt%, 20 wt%, and 25 wt%), which then dried under ambient room temperature conditions. The preparation of each sample coating involved the use of 50 mL of acrylic paint. This study focused on exploring the Cu content from 5 to 25 wt%, because adding Cu powder into a fixed 50 mL volume of acrylic paint proved practically difficult beyond this range. Trial after trial showed that Cu content above 25 wt% did not disperse well and increased viscosity, making it rather challenging to achieve uniform mixing.



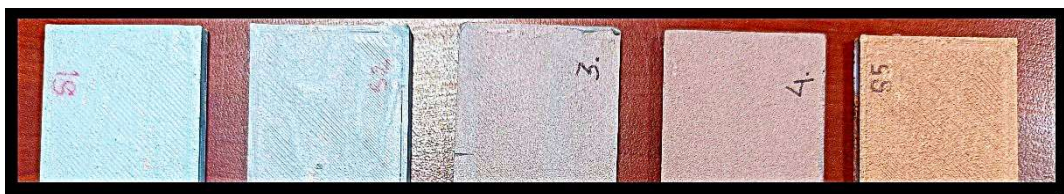
(a)



(b)



(c)



(d)

Figure 2. FDM-printed samples. (a) Sliced image for tensile sample; (b) tensile sample printed with ASTM D638 Type IV standard size; (c) Cu-coated sample; and (d) 15 × 15 mm samples of PLA coated with Cu powder for UV–Vis DRS and conductivity testing.

2.2. Mechanical Testing

Once the samples were ready for testing, the UTM machine for the tensile testing procedure, especially the ASTM D638 Type IV standard, was followed. The samples were tested at a constant deformation rate of 10 mm/min with a 5 kN capacity of the UTM machine (Make: Zwick Roell, Ulm, Germany). After mechanical testing reports for tensile stress, strain, and elongation at break were exported from the inbuilt software testXpert II version V3.6 of the UTM machine for further analysis, a procedure that has also been

practiced in previous studies [32,33]. The broken samples were photographed so that observations could be made on the type of failure near the failure region. Figure 3 shows the UTM testing setup with the fixed sample in the grip.



Figure 3. UTM testing setup with sample in grip.

2.3. SEM Analysis

The UTM-tested samples were further investigated under SEM using Carl Zeiss Sigma 500 FEG-SEM) (Make: ZEISS Microscopy; Oberkochen, Germany) for morphological analysis. The region near the PLA and acrylic/Cu-painted surface was subjected to SEM for a better understanding of the interface for its bonding and fracture phenomenon. For the fracture surface analysis, SEM microscopic images were captured with 200 \times , 500 \times , and 750 \times magnifications.

2.4. UV-Vis Diffuse Reflectance Spectroscopy

The 3D-printed and surface-coated samples of PLA/acrylic-Cu samples were subjected to UV-Vis DRS (make: Shimadzu; model: UV2600; Kyoto, Japan) analysis so that the sample absorbance and reflectance in the form of scattered IR energy could be analyzed. The samples were subjected to UV-Vis DRS analysis in the region of 200–800 nm wavelength.

2.5. Electrical Property Testing

The PLA samples were surface-coated with acrylic-Cu solution by using the low-energy technique of brush coating. Therefore, it was required to measure the electrical properties, such as capacitance and dissipation, and the dielectric constant of the material surface. For the dielectric constant and capacitance range analysis, a standard testing method was used. The testing machine consisted of a digital microcontroller-based capacitance meter capable of capacitance detection in the range of 01–6000 pF.

3. Results and Discussion

3.1. UTM Results and Discussion

The specimen, which went through to ASTM D638 Type IV testing, yielded noteworthy findings. Figure 4a shows the stress vs. strain graph for samples 1 and 5, the observed pattern for the mechanically tested samples of surface-coated PLA/ acrylic–Cu specimens. The graph depicted the significant rise of tensile strength for the increasing content of Cu in the acrylic paint layer on the PLA substrate. The rise in tensile strength of the specimen was observed to be gradual and linear from 13.5 MPa (sample 1) to 15.6 MPa (sample 5), whereas the percentage of strain at failure ranges from 4.2% (sample 1) to 8.6% (sample 5). The data points show a clear linear correlation between tensile strength and percentage Cu in acrylic paint layer, as evidenced by the trend line fitted through the data with the model R^2 value close to 98.56. The regression line has a positive gradient, indicating that there is a tendency for the tensile strength to grow as the percentage strain at failure increases. The observed rise in tensile strength appears to be uniform across all the data points. The data set represents the mean values for each sample, as three samples were tested for each setting for accuracy of experimentation.

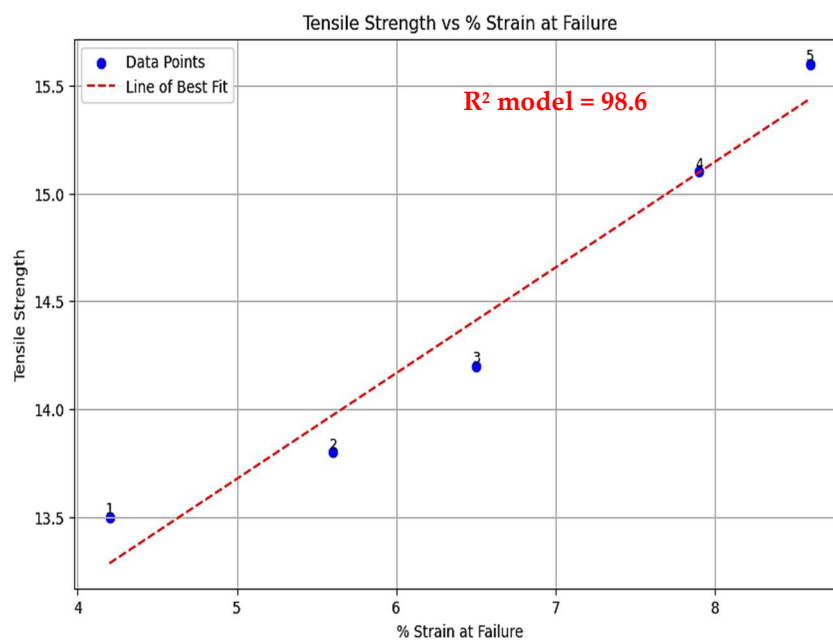
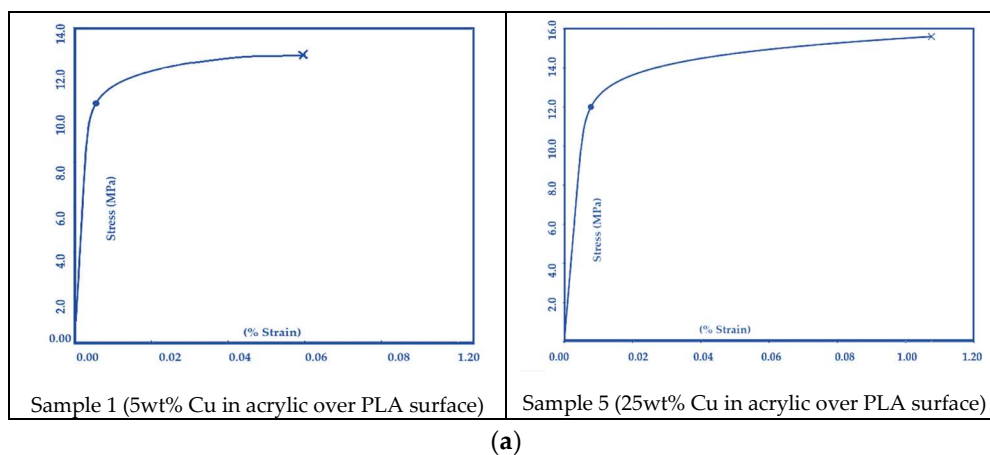


Figure 4. Cont.



Figure 4. (a) Tensile stress vs. strain data graph for samples 1 and 5; (b) best line of curve plot for tensile data for tested samples; (c) fractured sample under UTM testing; and (d) damaged profile of UTM specimen as per ASTM D638 Type IV standard.

The observed phenomenon wherein the tensile strength and percentage of strain at failure of the PLA/acrylic-Cu composite exhibit a positive correlation with percentage Cu in the acrylic paint layer is likely attributed to the surface coating present on the sample. Surface coatings are commonly employed to augment mechanical properties, particularly tensile strength, by furnishing supplementary structural reinforcement and shielding against external perturbations. Moreover, the surface coating may enhance interfacial adhesion between the polymer matrix and the reinforcing material (acrylic-Cu), thereby enhancing load transfer efficacy and mechanical characteristics, notably tensile strength. As the Cu content increases, the material might exhibit increased ductility, allowing the coated layer to deform more before failure.

When the specimen was reinforced with metallic particles in a polymeric matrix, prior investigations demonstrated that the specimen's mechanical strength was reduced in some cases [18,21,22]. Therefore, the current method of metallization has the potential to mitigate the decrease in the mechanical performance of polymeric samples when they are employed in conjunction with metallic fillers. Figure 4b,c show the damaged sample under UTM testing, which clearly shows the ductile nature of the acrylic-Cu surface coating as the sample was broken from the middle of the specimen, but the outer surface coating held the sample till the breakage of the outer surface layer of the acrylic-Cu layer. This may be the reason for the enhanced strain values of PLA/acrylic-Cu-coated samples.

Compared to traditional polymer-metal composites, the current fabrication method using an acrylic-Cu coating mitigates potential reductions in mechanical performance often seen with Cu-based metallic fillers in a polymeric matrix [10,18,21], ensuring better load transfer efficiency and structural integrity. This makes the material a promising candidate for structural applications requiring a balance between strength, flexibility, and durability. In comparison to existing polymer-metallic hybrid materials, the fabricated samples offer a novel approach by utilizing a surface-coating method instead of bulk metallic reinforcement, thereby preserving the lightweight nature of the polymer while enhancing its mechanical and optical performance.

3.2. Morphological Results and Discussion

3.2.1. SEM Results and Discussion

The fractured samples of UTM were further subjected to SEM analysis, and three different magnification ranges were selected for the analysis of the interface and different regions of the sample. Depicted in the SEM analysis, it is evident that the Cu powder particles are present in the acrylic–Cu surface-coating layer on PLA, as a clear difference between the two layers is visible (see Figure 5). From the SEM images, it may be observed that for the low-Cu-particle reinforced acrylic coating (sample 1: 5 wt% Cu in acrylic paint), the coating layer was torn out near the interface surface when stretched under the UTM machine. However, sample 8 (25 wt% Cu particle in acrylic paint) showed low damage near the interface layer. Similarly, it may also be observed that the Cu particles were densely distributed in sample 5 compared to sample 1, as there was clear evidence of a difference in color in the coating layer and a low proportion of Cu particles being observed under SEM analysis.

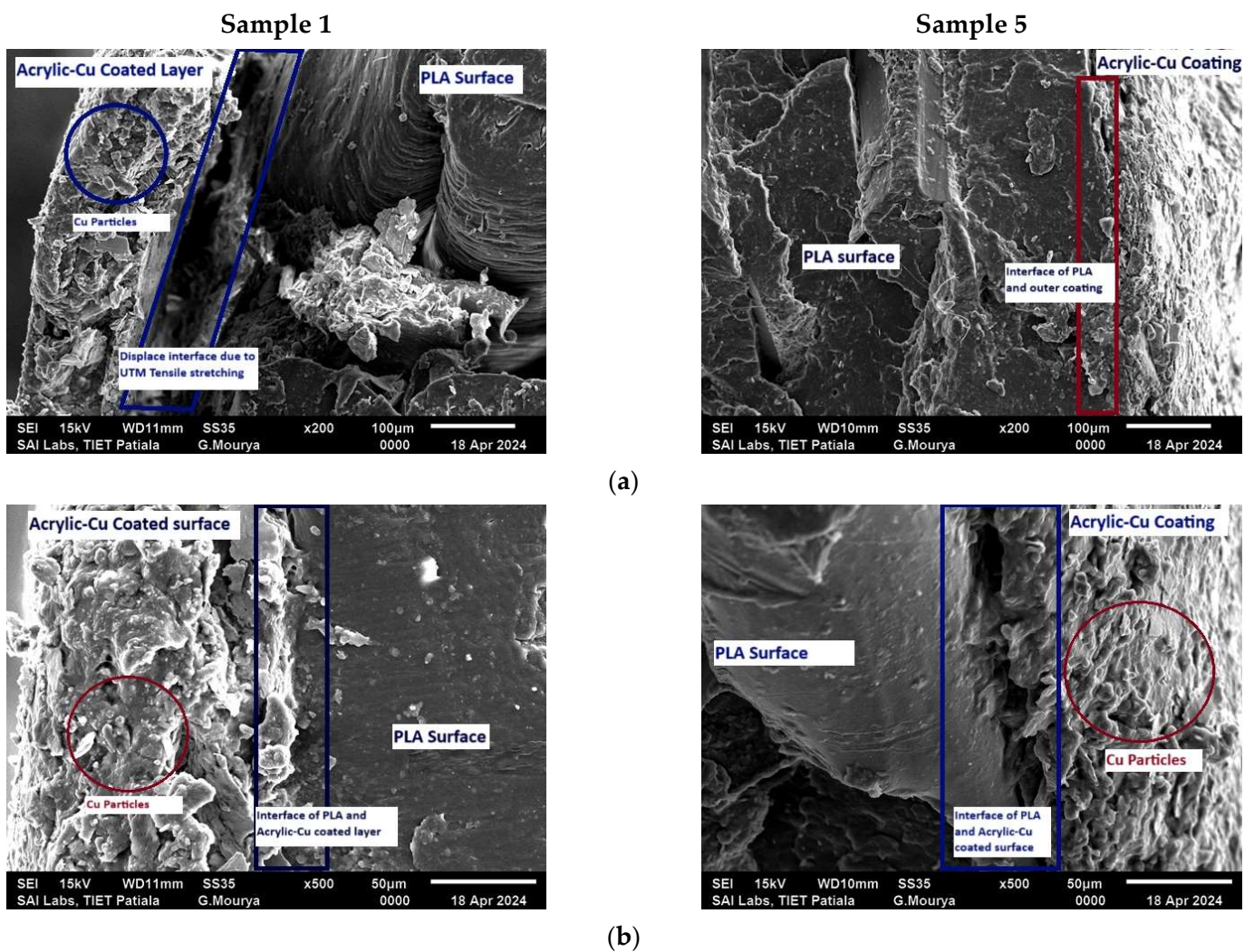
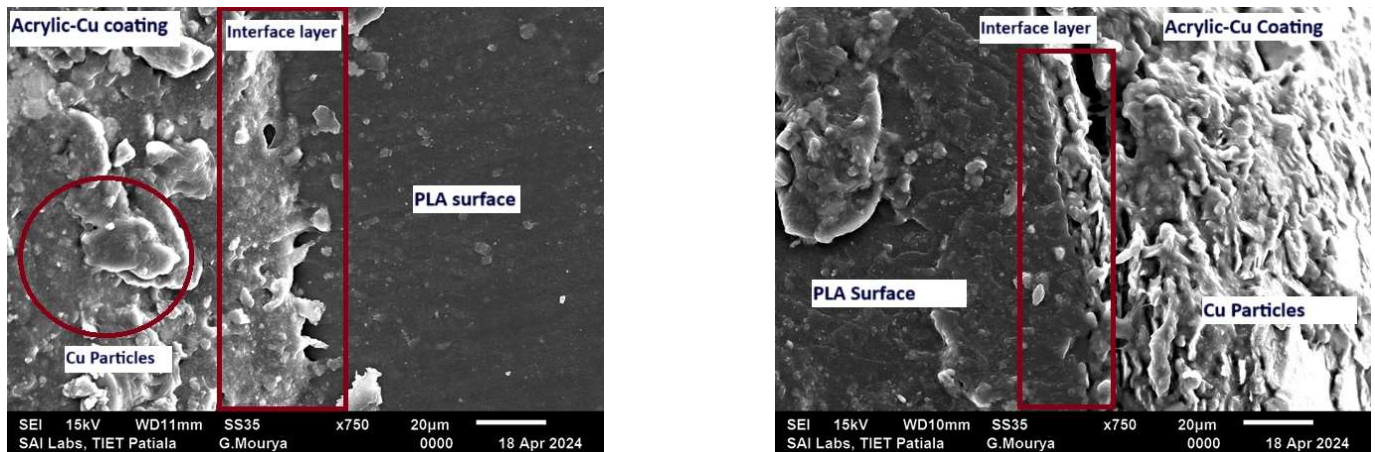


Figure 5. Cont.



(c)

Figure 5. SEM microscopic images for samples 1 and 5 at (a) $\times 200$, (b) $\times 500$, and (c) $\times 750$ magnification of analysis.

From Figure 5c, it may be observed that the coating layer of acrylic–Cu seems to be denser in sample 5 compared to sample 1. Samples 1 and 5 held Cu particles, as the presence of spherical Cu particles is evident in Figure 5; however, the particles were fully covered and were laminated by acrylic paint. No particle was free and activated on the surface of the specimen, due to which it may have a low electrical conductivity and dielectric constant.

3.2.2. UV–Vis Diffuse Reflectance Spectroscopy Results and Discussion

When examining the FDM-printed sample of PLA (size 15×15 mm) coated with acrylic–Cu solution at various ratios of Cu (5 wt% to 25 wt%), UV–Vis DRS offers valuable insights into the impact of copper on the surface’s light absorption and reflection properties. Researchers have reported the range of absorbance in the 250–150 nm wavelength region for neat/virgin PLA [34]. Based on the graph, it is evident that sample 1 (5 wt% Cu in acrylic paint on PLA surface) exhibits a UV–Vis DRS spectrum with a flat absorbance line in the 400–800 nm range (see Figure 6). There was a sudden increase in absorbance (0.4–1) observed in the wavelength region of 400 nm to 300 nm. When examining the UV–Vis spectrum, it becomes apparent that there are only slight variations compared to the pure PLA surface at this lower concentration of 5 wt% copper. It is possible that the acrylic–Cu layer could cause some absorption features in the UV region, potentially because of the presence of acrylic. However, the overall reflectance of the PLA substrate is likely to remain similar. Additionally, as the concentration of Cu increases, we noticed more significant alterations in the UV–Vis spectrum. There was an increase in the visibility of the absorption peaks associated with copper, resulting in a reduction in the reflectance levels across both the UV and visible regions.

As the level of Cu increased from 10 to 25 wt% (samples 2, 3, 4, and 5) in surface-coated PLA, there was a noticeable increase in the absorbance of UV rays in the 400–600 nm wavelength region. This increase was observed to be gradual, going from a level of 0.4 to 0.8. Following this, samples 2–5 exhibit a significant increase in absorbance (from 0.7 to 1.1) within the 300–400 nm wavelength range. Sample 5, containing 25 wt% Cu in the acrylic paint layer, exhibited the largest shift (see Figure 6) in the absorbance pattern compared to other specimens.

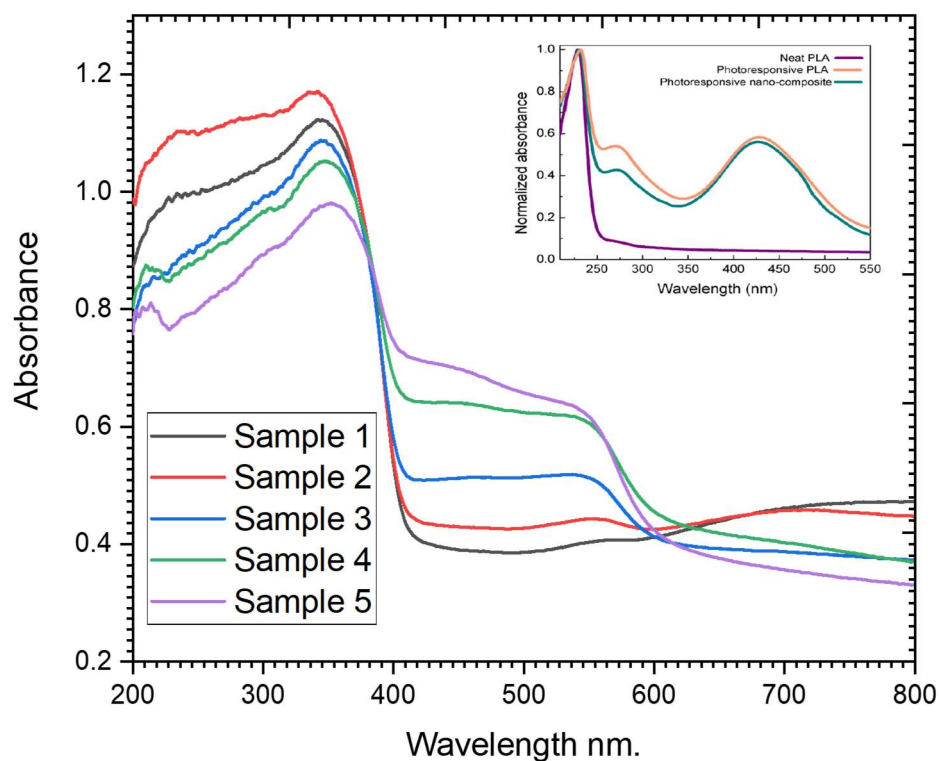


Figure 6. UV-Vis DRS graph for acrylic-Cu surface-coated PLA (Costanzo et al. (2014) [34]).

A systematic and progressive change in the optical response is observed as the copper content increases (10 wt% to 25 wt%). Such observations reveal that the absorption enhancement from 400–600 nm, together with absorption voraciousness in the 300–400 nm region, attests that with increased copper concentration, the aforementioned observations are rather pronounced in the interactions of light and matter at the surface. Copper-based compounds are generally characterized by strong absorption within the UV and the visible spectra caused by plasmonic effects, charge-transfer interactions, and intrinsic electronic transitions. The reduced intensity of reflectance across the above spectral ranges indicates an increased preference for absorption rather than for reflection, responsible for enhanced absorption contribution from surfaces. Considerable shifting of absorbance is observed, more specifically, at 25 wt% Cu (sample 5), which indicates that in light of the surface coating, there is a much greater degree of optical behavior imparted to the PLA substrate at that concentration. Increased absorption in the UV and visible ranges implies that with increased copper inclusion density in the acrylic matrix, light trapping may be enhanced due to more pronounced scattering and multiple internal reflections formulated in the coating. This may correlate to the formation of Cu-rich domains in the paint coat layer that lowers surface reflectance.

The consideration of this analysis has an enormous consequence in various applications requiring either controlled optical properties for UV protection, light attenuation, or enhanced absorption in functional coatings. The continuous progression and variation in copper concentration provide a venue for ameliorating customized surface coatings pertinent for directed light management applications. Future work regarding the details of the spectroscopic characterization, such as diffuse reflectance analyses and bandgap determination to un-wrap the exact influence of copper on the surface optical behavior, may now be entered.

4. Electrical Property Results and Discussion

In order to conduct a thorough analysis of the electrical properties, particularly the capacitance of the dielectric material created by surface-coating acrylic–Cu on the PLA substrate, samples measuring $10 \times 10 \text{ mm}^2$ were meticulously prepared and tested using a parallel plate setup. The test was conducted with a range of frequencies from 100 Hz to 1 MHz. Table 2 presents the capacitance results obtained for the PLA sample. Based on the samples, it can be observed that the capacitance of the samples is comparable to that of standard PLA samples. The capacitance is influenced by factors such as the thickness of the sample and the overall void fraction within the sample. Some of the studies have indicated that the capacitance of PLA can be enhanced with foreign fillers as well as with varying 3D printing parameters [35,36].

Table 2. Capacitance and dissipation values for acrylic–Cu surface-coated PLA substrate.

Sample	Capacitance	Dissipation
1	$6.96 \pm 0.42 \text{ pF}$	0.0399 ± 0.02
2	$7.80 \pm 0.95 \text{ pF}$	0.0626 ± 0.02
3	$6.82 \pm 0.06 \text{ pF}$	0.0057 ± 0.01
4	$7.40 \pm 0.33 \text{ pF}$	0.0720 ± 0.06
5	$5.70 \pm 0.23 \text{ pF}$	0.1316 ± 0.07
Pure PLA	$3.59 \pm 0.14 \text{ pF}$	0.0451 ± 0.03

It is important to mention that in the current study, the acrylic paint completely covered the Cu particles, as observed in the SEM analysis. As a result, the electrical capacitance values are relatively low, although the capacitance values increased up to 7.87 pF for (10 wt% Cu coating) from 3.6 pF for pure PLA. From the analysis, it may be observed that the coating results in an average capacitance value of 5–7 pF for the Cu-coated sample, which shows nearly a 100% increase in capacitance of the Cu-coated PLA samples. Table 2 provides information on the dissipation rate, which is a measure of the efficiency of energy storage and release in a capacitor. It indicates how effectively the capacitor can store and release energy without any loss of heat. Based on the dissipation rate, it is evident that as the Cu content increases, the dissipation value also increases, reaching a maximum of 0.13. The presence of Cu particles increased the capacitance efficiency of PLA, resulting in a reduction in loss values.

5. Conclusions

This study examines the metallization process on a surface created by 3D printing, utilizing a low-energy method. This entails utilizing an acrylic-paint-derived solution to strengthen the copper powder on the surface of a PLA substrate in order to assess the mechanical, morphological, absorbance, and capacitance characteristics of the created sample. The following are the observations:

1. From mechanical properties, it may be concluded that there is a significant rise in tensile strength for the increasing content of Cu in the acrylic paint layer on the PLA substrate. The rise in tensile strength of the specimen was observed to be gradual and linear from 13.5 MPa (sample 1) to 15.6 MPa (sample 5), whereas the percentage of strain at failure ranges from 4.2% (sample 1) to 8.6% (sample 5). The application of a surface coating on the samples, often employed to improve mechanical characteristics, can promote the even distribution of stress throughout the material, reducing the occurrence of localized vulnerabilities and enhancing the overall tensile strength.
2. SEM investigation detected the existence of copper powder particles in the PLA surface covered with acrylic–Cu. Sample 5, with 25 wt% Cu, showed the presence

of a dense layer of acrylic–Cu coating compared to sample 1. Furthermore, the acrylic paint formed a layer around the Cu particle, preventing the presence of any unbound Cu particles on the surface. This led to a reduced electrical conductivity and dielectric constant.

3. The UV–Vis DRS spectrum has a consistent absorbance level over the 400–800 nm range, followed by a sharp rise in absorbance within the 400 nm to 300 nm wavelength area. As the copper content rises, the absorption of UV radiation in the 400–600 nm wavelength range also increases, with the most significant change found in sample 5.
4. The capacitance values increased up to 7.87 pF for (10 wt% Cu coating) from 3.6 pF for pure PLA. From the analysis, it may be concluded that the coating results in an average capacitance value of 5–7 pF for the Cu-coated sample, which shows nearly a 100% increase in the capacitance of Cu-coated PLA samples.

Future Research

Future researchers could focus on optimizing the coating process to achieve a more uniform distribution of copper particles on the PLA substrate. Since the acrylic paint was found to laminate the copper particles, resulting in decreased electrical conductivity, future research could explore methods to improve the conductivity of the coated surface by activating the exposed surface. Furthermore, the work may be extended towards exploration of how variations in coating thickness, copper particle size, and concentration affect the dielectric constant and loss values of the material.

Author Contributions: Conceptualization, S.K. and P.T.; methodology, S.K. and P.T.; software, S.K.; validation, S.K., P.T. and S.S.R.K.; formal analysis, S.K., P.T. and S.S.R.K.; investigation, S.K.; resources, S.K. and S.S.R.K.; data curation, S.K.; writing—original draft, S.K.; writing—review and editing, S.K., P.T. and S.S.R.K.; visualization, S.K., P.T. and S.S.R.K.; supervision, S.K. and S.S.R.K.; project administration, S.K., P.T. and S.S.R.K.; funding acquisition, S.S.R.K. All authors have read and agreed to the published version of the manuscript.

Funding: This research received no external funding.

Data Availability Statement: The original contributions presented in this study are included in the article. Further inquiries can be directed to the corresponding authors.

Acknowledgments: The authors are highly thankful to the Thapar Institute of Engineering and Technology for continuous motivation and technical support.

Conflicts of Interest: The authors declare no conflicts of interest.

References

1. R. Kooloor, S.S.; Karimzadeh, A.; Abdullah, M.R.; Petru, M.; Yidris, N.; Sapuan, S.M.; Tamin, M.N. Linear-nonlinear stiffness responses of carbon fiber-reinforced polymer composite materials and structures: A numerical study. *Polymers* **2021**, *13*, 344. [[CrossRef](#)] [[PubMed](#)]
2. Shah, I.A.; Khan, R.; Kooloor, S.S.R.; Petru, M.; Badshah, S.; Ahmad, S.; Amjad, M. Finite element analysis of the ballistic impact on auxetic sandwich composite human body armor. *Materials* **2022**, *15*, 2064. [[CrossRef](#)]
3. Wong, K.J.; Johar, M.; Kooloor, S.S.R.; Petru, M.; Tamin, M.N. Moisture Absorption Effects on Mode II Delamination of Carbon/Epoxy Composites. *Polymers* **2020**, *12*, 2162. [[CrossRef](#)] [[PubMed](#)]
4. Kumar, S.; Singh, I.; Kumar, D.; Yahya, M.Y.; Kooloor, S.S.R. Mechanical and Morphological Characterizations of Laminated Object Manufactured 3D Printed Biodegradable Poly(lactic)acid with Various Physical Configurations. *J. Mar. Sci. Eng.* **2022**, *10*, 1954. [[CrossRef](#)]
5. Asghari, Y.; Mohammadyan-Yasouj, S.; Petru, M.; Ghandvar, H.; Kooloor, S.R. 3D Printing and Implementation of Engineered Cementitious Composites—A Review. *Case Stud. Constr. Mater.* **2024**, *21*, e03462.
6. Kumar, S.; Singh, I.; Kooloor, S.S.R.; Kumar, D.; Yahya, M.Y. On Laminated Object Manufactured FDM-Printed ABS/TPU Multimaterial Specimens: An Insight into Mechanical and Morphological Characteristics. *Polymers* **2022**, *14*, 4066. [[CrossRef](#)]

7. Vinay, D.L.; Keshavamurthy, R.; Erannagari, S.; Gajakosh, A.; Dwivedi, Y.D.; Bandhu, D.; Tamam, N.; Saxena, K.K. Parametric analysis of processing variables for enhanced adhesion in metal-polymer composites fabricated by fused deposition modeling. *J. Adhes. Sci. Technol.* **2023**, *38*, 331–354. [[CrossRef](#)]
8. Fijoł, N.; Aguilar-Sánchez, A.; Ruiz-Caldas, M.-X.; Redlinger-Pohn, J.; Mautner, A.; Mathew, A.P. 3D printed polylactic acid (PLA) filters reinforced with polysaccharide nanofibers for metal ions capture and microplastics separation from water. *Chem. Eng. J.* **2022**, *457*, 141153.
9. Sadeghian, H.; Ayatollahi, M.R.; Yahya, M.Y. Effects of copper additives on load carrying capacity and micro mechanisms of fracture in 3D-printed PLA specimens. *Theor. Appl. Fract. Mech.* **2023**, *127*, 104027.
10. Hasanzadeh, R.; Mihankhah, P.; Azdast, T.; Aghaiee, S.; Park, C.B. Optimization of Process Parameters of Fused Filament Fabrication of Polylactic Acid Composites Reinforced by Aluminum Using Taguchi Approach. *Metals* **2023**, *13*, 1013. [[CrossRef](#)]
11. Kam, M.; Saruhan, H.; İpekçi, A. Experimental investigation of vibration damping capabilities of 3D printed metal/polymer composite sleeve bearings. *J. Thermoplast. Compos. Mater.* **2022**, *36*, 2505–2522. [[CrossRef](#)]
12. Petousis, M.; Vidakis, N.; Mountakis, N.; Moutsopoulou, A.; Papadakis, V.; Maravelakis, E. On the substantial mechanical reinforcement of Polylactic Acid with Titanium Nitride ceramic nanofillers in material extrusion 3D printing. *Ceram. Int.* **2023**, *49*, 16397–16411. [[CrossRef](#)]
13. Yelamanchi, B.; MacDonald, E.; Gonzalez-Canche, N.; Carrillo, J.; Cortes, P. The fracture properties of fiber metal laminates based on a 3D printed glass fiber composite. *J. Thermoplast. Compos. Mater.* **2020**, *36*, 815–835.
14. Raichur, S.; Ravishankar, R.; Kumar, R.R. Tribological Studies of Nanoclay-Reinforced PLA Composites Developed by 3D Printing Technology. *J. Inst. Eng. Ser. D* **2024**, *105*, 517–525.
15. Mansour, M.T.; Tsongas, K.; Tzetzis, D. Carbon-Fiber- and Nanodiamond-Reinforced PLA Hierarchical 3D-Printed Core Sandwich Structures. *J. Compos. Sci.* **2023**, *7*, 285. [[CrossRef](#)]
16. Fijoł, N.; Mautner, A.; Grape, E.S.; Bacsik, Z.; Inge, A.K.; Mathew, A.P. MOF@Cell: 3D printed biobased filters anchored with a green metal-organic framework for effluent treatment. *J. Mater. Chem. A* **2023**, *11*, 12384–12394. [[CrossRef](#)]
17. Paz-González, J.A.; Velasco-Santos, C.; Villarreal-Gómez, L.J.; Alcudia-Zacarias, E.; Olivás-Sarabia, A.; Cota-Leal, M.A.; Flores-López, L.Z.; Gochi-Ponce, Y. Structural composite based on 3D printing polylactic acid/carbon fiber laminates (PLA/CFRC) as an alternative material for femoral stem prosthesis. *J. Mech. Behav. Biomed. Mater.* **2022**, *138*, 105632.
18. Ambruş, S.; Muntean, R.; Codrean, C.; Uțu, I.-D. Influence of printing conditions on the mechanical properties of copper-polylactic acid composites obtained by 3D printing fused deposition modelling. *Mater. Today Proc.* **2022**, *72*, 580–585. [[CrossRef](#)]
19. Bodaghi, M.; Sadooghi, A.; Bakhshi, M.; Hashemi, S.J.; Rahmani, K.; Motamedi, M.K. Glass Fiber Reinforced Acrylonitrile Butadiene Styrene Composite Gears by FDM 3D Printing. *Adv. Mater. Interfaces* **2023**, *10*, 2300337.
20. Mohammadi-Zerankeshi, M.; Alizadeh, R. 3D-printed PLA-Gr-Mg composite scaffolds for bone tissue engineering applications. *J. Mater. Res. Technol.* **2022**, *22*, 2440–2446.
21. Sharifi, J.; Paserin, V.; Fayazfar, H. Sustainable direct metallization of 3D-printed metal-infused polymer parts: A novel green approach to direct copper electroless plating. *Adv. Manuf.* **2024**, *12*, 784–797.
22. Kumar, R.; Kumar, M.; Chohan, J.S.; Singh, N.K.; Mahajan, D.K. Corrosion and Thermal Analysis of 316L Stainless Steel Coated PLA Parts Fabricated by FDM Process for Biomedical Applications. *Prot. Met. Phys. Chem. Surf.* **2023**, *59*, 736–749. [[CrossRef](#)]
23. Moraczewski, K.; Trafarski, A.; Karasiewicz, T.; Mazurkiewicz, M.; Szabliński, K.; Augustyn, P.; Rytlewski, P. Copper electroless metallization of 3D printed poly(lactide acid) elements via tannic acid or polydopamine coatings and silver catalyst. *Mater. Today Commun.* **2023**, *34*, 105332.
24. Inclán-Sánchez, L. Performance Evaluation of a Low-Cost Semitransparent 3D-Printed Mesh Patch Antenna for Urban Communication Applications. *Electronics* **2023**, *13*, 153. [[CrossRef](#)]
25. Aziz, M.; El Hassan, A.; Hussein, M.; Zaneldin, E.; Al-Marzouqi, A.H.; Ahmed, W. Characteristics of antenna fabricated using additive manufacturing technology and the potential applications. *Heliyon* **2024**, *10*, e27785. [[PubMed](#)]
26. Farajian, J.; Hatami, O.; Bakhtiari, M.; Darabinajand, B.; Mahboubkhah, M. Investigation of Mechanical Properties of 3D-Printed PLA Coated with PU/MWCNTs in a Corrosive Environment. *Arab. J. Sci. Eng.* **2024**, *49*, 11181–11193.
27. Ekonomou, S.I.; Soe, S.; Stratatos, A.C. An explorative study on the antimicrobial effects and mechanical properties of 3D printed PLA and TPU surfaces loaded with Ag and Cu against nosocomial and foodborne pathogens. *J. Mech. Behav. Biomed. Mater.* **2022**, *137*, 105536.
28. Moradi, M.; Dezaki, M.L.; Kheyri, E.; Rasouli, S.A.; Attar, M.A.; Bodaghi, M. Simultaneous FDM 4D printing and magnetizing of iron-filled polylactic acid polymers. *J. Magn. Magn. Mater.* **2023**, *568*, 170425.
29. Sukindar, N.A.; Yasir, A.S.H.M.; Azhar, M.A.M.; Halim, N.F.H.A.; Sulaiman, M.H.; Sabli, A.S.H.A.; Ariffin, M.K.A.M. Evaluation of the surface roughness and dimensional accuracy of low-cost 3D-printed parts made of PLA-aluminum. *Heliyon* **2024**, *10*, e25508.
30. Alzyod, H.; Takacs, J.; Ficzer, P. Improving surface smoothness in FDM parts through ironing post-processing. *J. Reinf. Plast. Compos.* **2023**, *43*, 671–681. [[CrossRef](#)]

31. Amin, M.; Singh, M.; Ravi, K. Fabrication of superhydrophobic PLA surfaces by tailoring FDM 3D printing and chemical etching process. *Appl. Surf. Sci.* **2023**, *626*, 157217. [[CrossRef](#)]
32. Abdi, B.; Koloor, S.S.R.; Abdullah, M.R.; Amran, A.; Yahya, M.Y. Effect of strain-rate on flexural behavior of composite sandwich panel. *Appl. Mech. Mater.* **2012**, *229*, 766–770. [[CrossRef](#)]
33. Joshani, M.; Koloor, S.; Abdullah, R. Damage Mechanics Model for Fracture Process of Steel-Concrete Composite Slabs. *Appl. Mech. Mater.* **2012**, *165*, 339–345. [[CrossRef](#)]
34. Costanzo, G.D.; Ribba, L.; Goyanes, S.; Ledesma, S. Enhancement of the optical response in a biodegradable polymer/azo-dye film by the addition of carbon nanotubes. *J. Phys. D Appl. Phys.* **2014**, *47*, 135103. [[CrossRef](#)]
35. Thangavel, S.; Ponnusamy, S. Application of 3D printed polymer composite as capacitive sensor. *Sens. Rev.* **2019**, *40*, 54–61. [[CrossRef](#)]
36. Kuzmanić, I.; Vujović, I.; Petković, M.; Šoda, J. Influence of 3D printing properties on relative dielectric constant in PLA and ABS materials. *Prog. Addit. Manuf.* **2023**, *8*, 703–710. [[CrossRef](#)]

Disclaimer/Publisher’s Note: The statements, opinions and data contained in all publications are solely those of the individual author(s) and contributor(s) and not of MDPI and/or the editor(s). MDPI and/or the editor(s) disclaim responsibility for any injury to people or property resulting from any ideas, methods, instructions or products referred to in the content.